Mausam, (1985), **36**, 4, 417-422

551.510.52 : 551.553.21

The thermodynamic and kinematic structure of the troposphere over the Arabian Sea and the Bay of Bengal during 1979 monsoon season

T.K. RAY and H.S. BEDI

Meteorological Office, New Delhi

(*Received 24 January 1984*)

सार — मानसून प्रयोग (मोनैक्स-79) ने 1979 के मानसून के दौरान भारतीय समुद्र क्षेत्रों के ऊपर के विस्तृत आंकड़े प्रदान किए हैं। सोवियत संघ के अनुसंधान पोतों ने अरब सागर तथा बंगाल की खाड़ी के ऊपर बने स्थिर बहुभुजों में उपरितन वायु आंकड़े रिकार्ड किए हैं। इन आंकड़ों का उपयोग करते हुए 1000 से 100 मिलिबार दाब तक वायु मण्डल की शुद्ध गतिक तथा ऊष्मा गतिक संरचना के निर्धारक परिमापक अभिकलित किए गए। मानसून के विभिन्न चरणों में इन परिमापकों की तुलना की गई तथा इनसे अरब सागर व बंगाल की खाड़ी के ऊपर मानसून के आरम्भ, सक्रियता तथा व्यवधान अवधियों से संबंधित दिलचस्प विशेषतामास सामने आए।

ABSTRACT. The Monsoon Experiment (MONEX-79) has provided an exhaustive data set over the Indian seas during 1979 monsoon. The USSR research ships recorded upper air data in stationary polygons formed over the Arabian Sea and the Bay of Bengal. Using these data various parameters determining the kinematic and thermodynamic structure of the atmosphere from 1000 to 100 mb have been calculated. The comparison of these parameters during various phases of the monsoon over the Arabian Sea and the Bay of Bengal brings out interesting contrasts during the onset, active and break monsoon periods.

1. Introduction

A number of studies have been made on the role of southern hemisphere in the genesis of southwest monsoon, Rao (1964), Pisharoty (1965), Findlater (1969) and Saha (1970) observed a strong cross equatorial air flow from southern to northern hemisphere near the Somalia coast during southwest monsoon. Pisharoty (1965), Sikka and Mathur (1965), Saha (1970) and Saha and Bavadekar (1973) also noticed the cross equatorial water vapour fluxes associated with southwest monsoon. Rao and Desai (1971) tried to re-establish that the southwest monsoon owes its origin to the southern hemispheric trades which get deflected at the equator and approach the western coast of India as monsoon. From an estimation of vapour transport across equator over the Arabian Sea led Pisharoty (1965) to conclude that bulk of the water vapour supply during monsoon over India is of northern hemispheric origin. However, the later study by Saha and Bavadekar (1973) has shown that the net cross equatorial flux of water vapour is only about 30% larger than the evaporation over the Arabian Sea. Based on larger data sets collected during Indo-Soviet Monsoon Experiment 1973 (ISMEX-73) Ghosh *et al.* (1978) confluded that the Arabian Sea plays a dominant role in supplying the moisture to the southwest monsoon over India. They also postulated a zonal cell with ascending limb over the west coast of India and descending one over the western Arabian Sea. A similar cell with ascending limb over the northeast India and subsiding limb over the northwest India was earlier proposed by Das (1962).

Thus we see that the relative countribution of the Arabian Sea towards the southwest monsoon in terms of supply of water vapour, heat and mass fluxes still appears to be an open question. Same is the case with the Bay of Bengal.

The present study based on data collected during Monsoon Experiment of 1979 (MONEX-79) is aimed at further investigating the role of the Arabian Sea and the Bay of Bengal during the southwest monsoon.

2. Data and analysis

During MONEX-79 (1 May 1979 to 31 August 1979), the USSR ships were in stationary polygons on following days

Polygon I : 16 to 29 May 1979

Polygon II : 2 to 14 June 1979

Polygon III : 10 to 23 July 1979

The first two polygons were in the Arabian Sea and the third one in the Bay of Bengal. The geographical location of each of these polygons along with ship positions is shown in Fig. 1. Polygon I was planned to cover the pre-onset phase of monsoon, polygon II the onset and advance of monsoon over

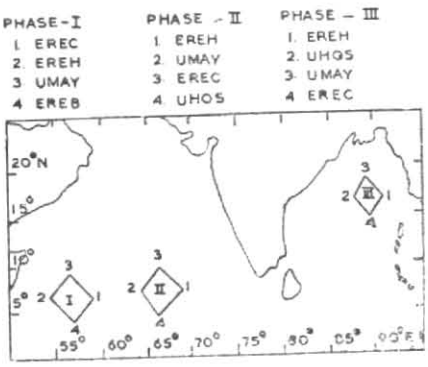

Fig. 1. Stationary polygons

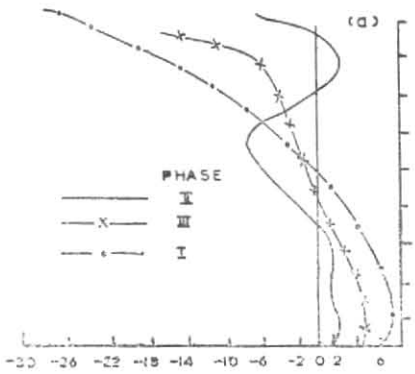

Fig. 2(a). Zonal winds (mps)

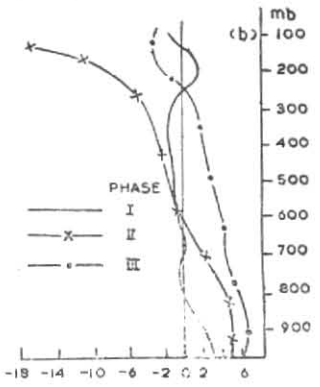

Fig. 2(b). Meridional winds (mps)

the Arabian Sea and polygon III the active monsoon phase over the Bay of Bengal. Table 1 gives the scientific objective planned to be studied by these polygons and a brief summary of synoptic situations actually encountered during each phase. The MONEX-79 research ships in their stationary positions provided very valuable set of data on the atmospheric structure over the Arabian Sea and the Bay of Bengal. In all, these data consist of over 600 upper air soundings from research ships in these stationary polygon positions and have been utilised in this study. From the data at standard and significant levels, the geopotential height, dry bulb and dewpoint temperatures, zonal and meridional components of wind were interpolated at 25 mb intervals between 1000 and 100 mb, thus, giving data over 37 levels for each sounding. Observations were taken at main synoptic hours : 00, 06, 12 and 18 GMT. At each of these levels horizontal divergence and vertical component of relative vorticity were calculated as flux and circulation per unit area respectively over the polygonal region.

Total flux and circulation were calculated by contour integration over the polygon as follows :

$$\text{flux} = \oint v_n \, dl = \sum_{i=1}^{4} \bar{v}_{ni} \, l_i$$

$$\text{Circulation} = \oint v_r \, dl = \sum_{i=1}^{4} \bar{v}_{ri} \, l_i \qquad (1)$$

where $\bar{v}_{ni}$ and $\bar{v}_{ri}$ are the mean normal and radial component of wind over the ith side of the polygon and l_i is the length of the side. To get proper sign for vorticity, integration was performed in an anticlockwise direction. In a few cases, when the data from only three ships were available such integration was performed over the triangle. If data were available from less than 3 ships, they were not considered for the analysis.

Vertical velocity (ω) was obtained by vertical integration of divergence equation as,

$$\omega = \int_{1000}^{p_i} \nabla \cdot \mathbf{v} \, dp + \omega_o \qquad (2)$$

The lower boundary condition was $\omega_0 = 0$ and the imposed upper boundary condition was taken as $\omega_{100} = 0$ at 100 mb. This was achieved by adjusting the divergence at each level following O' Brien (1970) so that the total divergence between 1000 and 100 mb is zero. While doing such adjustments the residual divergence was distributed among the levels proportional to the mean wind speed at various levels.

Other parameters calculated were the kinetic energy, dry and moist static energy, precipitable water, zonal and meridional transport of water vapour and divergence of water vapour as follows :

1. Dry static energy (SSD) $= gh + c_p T$, c_p specific heat at conatant pressure.
2. Moist static energy $= SSD + q.Le$, Le latent heat of evaporation.
3. Precipitable water $= \dfrac{1}{g} \displaystyle\int_{1000}^{100} q \, dp$
4. Zonal transport of water vapour $= \dfrac{1}{g} \displaystyle\int_{1000}^{100} \bar{q} \, \bar{u} \, dp$
5. Meridional transport of water vapour $= \dfrac{1}{g} \displaystyle\int_{1000}^{100} \bar{q} \, \bar{v} \, dp$
6. Divergence of water vapour $= \nabla . q \, \bar{\mathbf{v}} \, dp$
7. Mean Kinetic energy $KE = \frac{1}{2} (\bar{u}^2 + \bar{v}^2)^{\frac{1}{2}}$

Where u,v are the zonal and meridional components of wind V, T is temperature. q specific humidity and h is the geopotential height. The over bar indicate the polygonal mean of the parameters.

Computations of the above and other derived parameters were made for the four synoptic hours everyday from which time averages were calculated. For economy of space all the graphs and charts have not been presented but only selected ones have been produced.

An examination of the actual synoptic situations during polygon I (16-29 May) showed that equatorial trades intensified and the low level anticyclone weakened and moved away southwards. During the

TABLE 1

Scientific objectives and synoptic Summary

Scientific objective	Summary of synoptic situations
Polygon I (6.3° N, 57.0°E : West Arabian Sea) 16-29 May 1979	
To study the vertical structure of atmosphere over the western Arabian Sea during the pre-onset phase	Low level anticyclone centred around 5° N/65° E was preodminant in the beginning but weakened and shifted southwards towards the end period. Weak southwesterly wind prevailed over Somalia coast. Subtropical jet stream was running between 25° and 30° N.
Polygon II (7.0° N, 67.0°E: Central Arabian Sea) 2-14 June 1979	
To study the onset of monsoon over the Arabian Sea	Low level anticyclone disappeared on 5 June and cross-equatonal flow along Somalia coast increased. Upper tropospheric ridge established at 200 mb and elongated. Monsoon current started establishing over the Arabian Sea from 9 June. Subtropical westerly jet shifted northward to 40° N over Indian longitudes. Tropical easterly jet appeared over south India. Somali jet started to form toward the end of the period.
Polygon III (16·0° N, 89.5° E : North Bay of Bengal) 10-23 Jul' 79	
To study the atmospheric structure over the Bay of Bengal during active monsoon phase including formation and movement of monsoon depressions and breaks in monsoon	Monsoon trough shifted northwards from its normal position, reaching foot hills by 17 July. No Bay depression formed during the period, though a feeble low pressure formed over north Bay on 13th and weakened later. Tropical easterly jet broadened and no distinct maxima could be traced. Somalia jet was also weak during the period. Subtropical jet ran between 40° N and 45° N. Break monsoon conditions started on 17 July and continued till the end of the period.

period of polygon II (2-14 June) we see that the low level anticyclone disappeared and cross-equatorial flow across equator increased. Monsoon flow with 10-20 kt southwesterlies established over south Bay of Bengal. One weak low pressure wave entered Bay through Burma on 5 June and weakened. Later a cyclonic circulation appeared over head Bay of Bengal but soon weakened. The third stationary polygon represents basically the atmospheric conditions, over Bay of Bengal, associated with break monsoon conditions. The anticyclogenesis in the equatorial air was observed around 17 July, heralding 10 day long break monsoon. Towards the end of the phase the monsoon trough could be seen to shift from its northern position southwards indicating revival of monsoon.

3. Results

3.1. *Upper winds*

At polygon I, upto 20 May, the low level flow was light southwesterly or northerly. From 21 May, the westerly component strengthened reaching its maximum value on 24 May. Higher level flow was northwesterly throughout this phase. The average wind profiles for the four hours show 2-3 mps zonal westerlies upto 650 mb [Fig. 2(a)]. These change to easterlies having a maximum strength of 8 mps near 400 mb. Above this level a narrow zone of westerlies is observed between 275 mb and 125 mb. Southerlies extend upto 850 mb. Beyond this level very weak northerlies prevail upto 250 mb with a maximum strength of 2-3 mps near 300 mb. Between 250 and 150 mb against a narrow zone of southerlies is noticed.

Towards the beginning period of phase II, west-northwesterlies were concentrated in the lower layers. From 5 June the low level flow became westsouth-westerly, strengthend and deepened reaching maximum depth upto 350 mb between 9 & 11 June. Except this three day period of deep westerlies, the upper level flow was generally eastnortheasterly or eastsouth-easterly. The average meridional wind is shown in Fig. 2 (b). In the mean, the westerlies prevailed upto 600 mb, and easterlies aloft. Easterlies reached their maximum strength of 18 mps at 125 mb. As for the meridional component, weak southerlies prevailed upto 250 mb and weak northerlies aloft.

In the beginning of phase III, southwesterlies with strength 12-14 mps prevailed upto 350 mb. The southwesterlies, weakened and decreased in depth continuously till the end of the phase and during the break monsoon conditions. The spectacular weakening and narrowing in depth of westerly component during this phase is seen in Fig. 3. In the mean during this phase the westerlies extended upto 550 mb with maximum strength of 8 mps around 850 mb. The easterlies aloft reached a maximum strength of 35 mps at 100 mb. Looking at the meridional component, southerlies are noticed upto 300 mb and northerlies aloft. Strongest southerlies (4-5 mps) are at the lowest level and the strongest northerlies (4-6 mps) at 150 mb.

3.2. *Temperature distribution*

The vertical thermal structure during all the phases is essentially similar, except that temperatures during phase II are more by about 1 deg. C than during phase I particularly in the middle and upper troposphere. Temperatures for phase III are also more than those for phase II nearly by the same amount. Individual hourly temperature distribution showed that 06 and 12 GMT temperatures were slightly higher than those from 00 and 18 GMT throughout the atmosphere. Freezing level (0 deg. C) for all hours lay around 550 mb during all the three phases.

3.3. *Kinetic energy*

Fig. 4 (a) shows vertical distribution of kinetic energy during the three phases. The kinetic energy profiles for individual hours did not show any appreciable diurnal variations. Hence only mean daily profile of kinetic energy is presented. During phase I, kinetic energy maximum is observed around 400 mb associated with strong easterly flow at this level. A minor maximum associated with upper westerly flow occurs around 175 mb. Kinetic energy is minimum around 650 mb where low level westerly flow changes to upper level easterly flow. During phase II and III Kinetic energy is nearly constant (15-20 m^2 sec^{-2}) for phase II and nearly double of it for phase III) upto 300 mb and 500 mb respectively and increased asymptotically thereafter reaching a maximum value

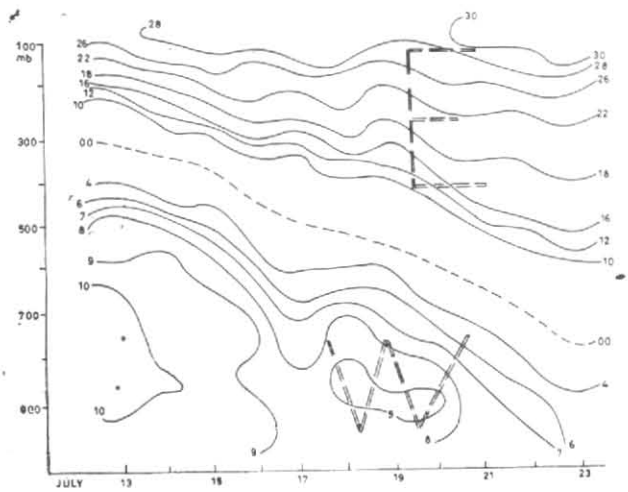

Fig. 3. Daily average zonal winds (mps)

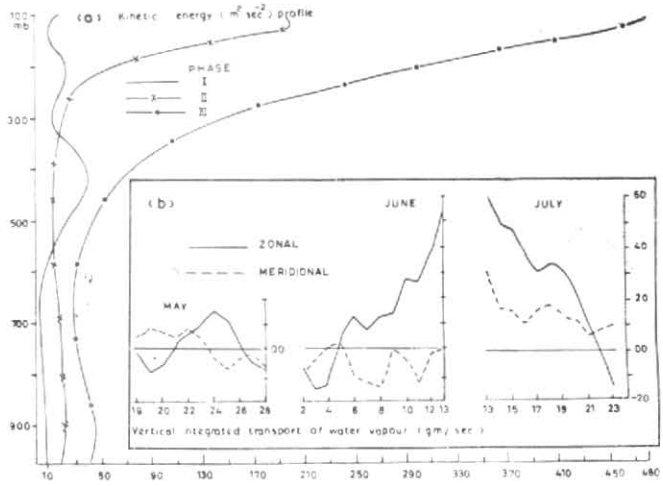

Figs. 4(a&b)

of 180 m^2 sec^{-2} during phase II and of 480 m^2 sec^{-2} during phase III at 100 mb. The 100 mb being the highest level considered in the study, the maximum apparently is situated at a still higher level.

3.4. *Water vapour*

3.4.1. *Precipitable water*

The vertical distribution of mean specific humidity (gm/kg) for the three phases does not show much except the fact that there is increase in specific humidity from phase I to phase II to phase III by about 1 gm/kg throughout the depth upto about 350 mb.

The daily variations of moisture in terms of total precipitable water integrated upto 100 mb have been computed but for reasons of space the diagram is not presented here. The main feature of precipitable water distribution during phase I is a steady increase in its amount from 4 gm to 5 gm between 18 and 21 May. Thereafter it continued nearly at the same level till the end of the phase. Total precipitable water during the beginning of phase II was about 5 gm and increased steadly to 6 gm towards the end of the phase. During phase III precipitable water was about 6 gm, with fluctuation between 5 and 7 gm. An important feature is the decrease in precipitable water between 18 and 21 July coinciding with early part of break monsoon period. However, from 22 July onwards precipitable water started increasing about 5 days prior to conclusion of break monsoon condition on 27 July.

3.4.2. *Transport of water vapour*

Vertically integrated zonal and meridional transport of water vapour are shown in Fig 4(b). During phase I water vapour transport is towards northwest during first four days, but thereafter with the southward shift of low level anticyclone it becomes southeastwards. In the beginning of phase II water vapour transport was southwestwards but from 5 June onwards southeastward transport of water vapour started as the Arabian Sea flow started organising before the onset of monsoon which took place towards the end of the phase. During phase III there was northeastward moisture transport throughout the period with a steady decrease in its magnitude with time, particularly of zonal transport.

3.5. *Static energy — dry and moist*

Mean static energy distribution (Fig. 5) does not reveal much of a variation among the three phases except the fact that both dry and moist energies at each level are higher than the corresponding values in the preceding phase. Dry static energy increases almost lineraly with height from 72.5 m^2 sec^{-2} at 1000 mb to 83.5 m^2 sec^{-2} at 100 mb during all the three phases. At different levels the dry static energy marginally increased from phase I to phase III through phase II. The moist static energy initially at 83-84m^2 sec^{-2} at 1000 mb decreases to 79–80 m^2 sec^{-2} at 550 mb, then again it increases to 83–84m^2 sec^{-2} at 100 mb. Moist static energy varies rather widely among the three phases as compared to dry static energy. Nitta (1980) also observed similar vertical profile of dry and moist static energy for phase III.

3.6. *Horizontal flux of water vapour*

For reasons of space only 1200 GMT horizontal flux of water vapour ($\nabla \cdot q\,v$) is presented in Fig. 6. During phase I we observe divergence at lower layers upto 800-850 mb and convervence above these levels at 00 and 12 GMT. At 06 GMT the reverse order, *i.e.*, moisture convergence is noticed at lower levels and divergence aloft. The water vapour fluxes at 1800 GMT are very weak as compared to other hours. During phase II the patterns of horizontal vapour flux is similar to that during phase I, *i.e.*, at 00, 12 and 18 GMT there is general vapour divergence at lower levels and convergence aloft, while at 06 GMT this pattern gets reversed. The vertical distribution of water vapour flux during phase III is very systematic and similar at all hours. Over a very shallow lower layer upto 900 mb water vapour divergence is noticed. Above this layer upto about 650 mb strong water vapour convergence takes place which has highest value around 750 mb. Above 600 mb there is again divergence of water vapour with maximum value reaching around 400 mb.

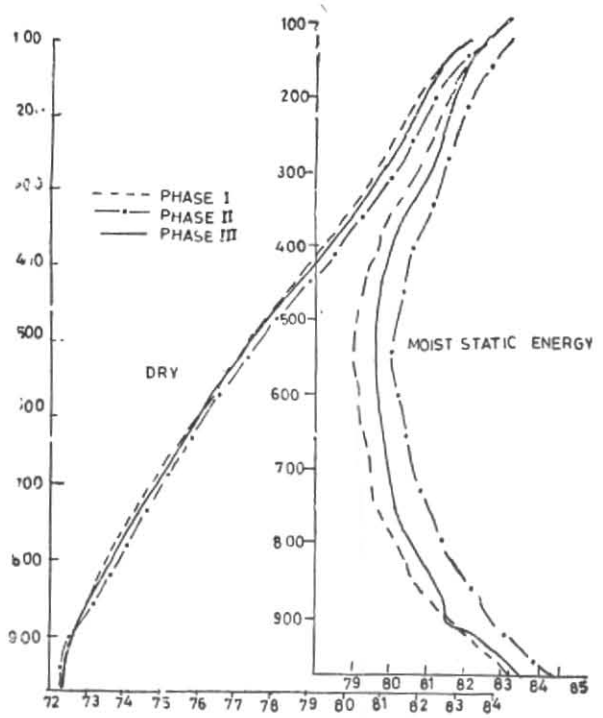

Fig. 5. Static energy: dry & moist (m^2/sec^2)

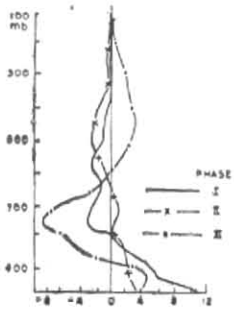

Fig. 6. Water vapour flux (gm/gm/sec) [unit : 10^{-8}]

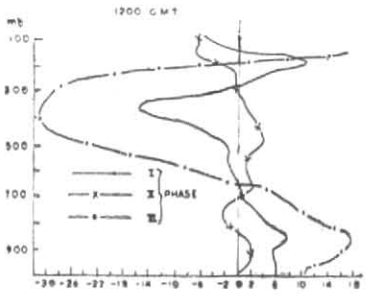

Fig. 7. Relative vorticity (unit : 10^{-6})

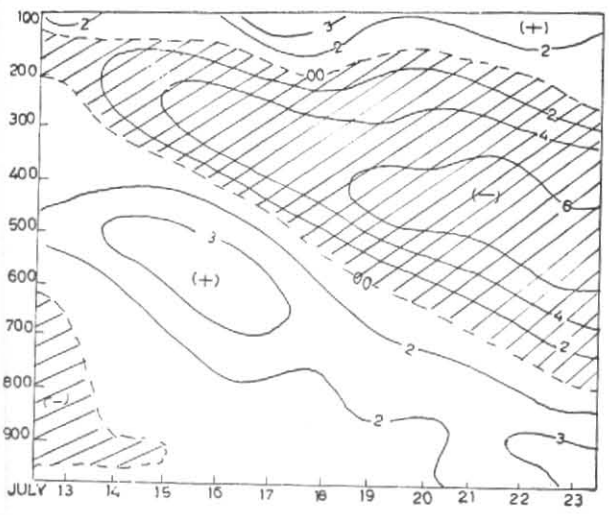

Fig. 8. Daily variation of relative vorticity 10^{-5} during break monsoon

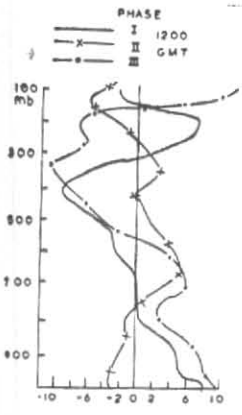

Fig. 9. Divergence (unit : 10^{-6} sec^{-1})

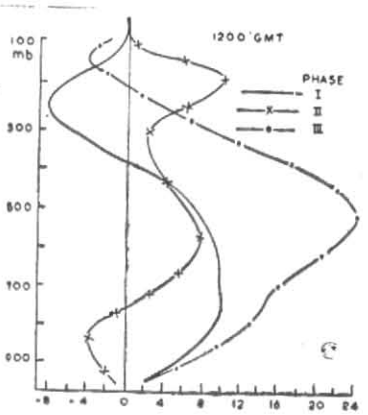

Fig. 10. Vertical velocity (unit : 10^{-4} mb/sec)

3.7. *Relative vorticity*

Fig. 7 shows vertical distribution of average relative vorticity for 00, 06, 12 and 18 GMT for the three phases. During phase I we observe positive vorticity over the lower layers of the atmosphere at all the four hours, though vertical extent of the positive vorticity shows large diurnal variations. At 00 GMT the vorticity is positive upto 500 mb becoming negative between 475 mb and 275 mb. Above this level vorticity becomes positive again. Vertical distribution of vorticity at 12 GMT also shows nearly similar pattern though at this hour the extent of negative vorticity over the middle layers is much larger. At 0600 GMT vorticity is positive only upto 750 mb and negative throughout the upper layers. At 1800 GMT the depth of low level positive vorticity becomes very shallow. During phase II, the relative vorticity pattern for four hours show large variations. This ship polygon was at the onset phase of the monsoon. Sudden changes in atmospheric flow features could have resulted in large diurnal variation of the vorticity. During this phase also we generally notice positive vorticity in the lower and middle layers and negative vorticity in the upper layers, though there are large diurnal variations in the vertical extent of such distribution. Vorticity distribution during phase III is very systematic and typical of dynamically active atmosphere. The lower atmosphere upto about 600 mb is seen to have positive vorticity. The layer from 500 mb to 200 mb has negative vorticity, 300 mb level having the minimum negative vorticity. Above 200 mb vorticity again becomes positive. Fig. 8 shows the daily variations of relative vorticity during phase III. It is interesting to note the continuous reduction in the depth of layer of positive vorticity at the lower level and increasing negative vorticity at the upper levels during the break monsoon period.

3.8. *Divergence*

Fig. 9 shows the distribution of vergence. Although there is sufficient diurnal variation in the divergence patterns, some significant features are apparent in its distribution. All the three phases have dominantly divergent field at the lower levels. During phase I,

tht level between 750 and 650 mb is found to be the level of 'non-divergence'. Between 650 and 300 mb convergence dominates; maximum convergence occurring around 350 to 400 mb levels. At upper levels again divergence is noticed. During phase II, weak divergence or convergence is noticed at lower levels upto 800 mb. Between 850 and 600 mb generally divergence occurs with its maximum value around 700 mb. Between 600 and 300 mb levels again weak divergence/convergence is noticed. At higher levels convergence is noticed beyond 300 mb with its maximum occurring around 200 mb. The divergence field for phase III represents break monsoon conditions. The lower troposphere upto 500 mb is dominated by sufficiently strong divergence; in case of 00 and 12 GMT, convergence is noticed between 800 and 600 mb. Vergence values are minimum around 500 mb which could be regarded as level of non-divergence. Beyond this level convergence is noticed upto about 150 mb, with maximum convergence taking place around 200 mb level. At higher levels the field again becomes divergent. An examination of daily divergence field showed progressive decrease in convergence over lower layers (800-600 mb) and deepening of the layer of upper level convergence with the approach and during break monsoon conditions.

The divergence field during all the three phases represents weak monsoon conditions. Another important feature noticed is the level of non-divergence which at the west Arabian Sea during phase I is around 700 mb shifts to 500 mb at the north Bay of Bengal during phase III.

3.9. *Vertical velocity*

The distribution of vertical velocity during three phases can be seen in Fig. 10. During phase I, downward motion dominates the lower troposphere upto about 450 mb, except for 18 GMT which shows upward vertical motion at all the levels. The reason for such difference in vertical velocity at 18 GMT and other hours is not clear. A careful examination of the initial and derived data could not reveal any error. In the upper trosphere generally upward motion is noticed. Phase II is dominated by weak downward motion at all levels at 06 and 18 GMT while at 00 and 12 GMT upward motion is noticed upto 700 mb levels and downward vertical velocity aloft. During phase III downward vertical motion is noticed upto 200 mb at 06, 12 and 18 GMT. The strongest downward motion is noticed between 500 and 300 mb levels. The vertical velocity field at 00 GMT is rather weak though in this case also downward motion dominates the lower layers. An examination of daily vertical velocity patterns during phase III showed that the strongest downward vertical motion in the middle troposphere occurred during the break monsoon period starting from 17 July.

4. Conclusion

The 1979 summer monsoon was a typically weak monsoon practically throughout the country. The thermodynamical and kinematic structure brought out above on the basis of data collected by research ships thus correspond to general weak monsoon conditions. The first phase during the pre-onset phase shows rather weak flow with dominantly subsiding motion and low moisture contents over the Arabian Sea. The second phase shows increase in kinetic energy as well as moisture contents and rising motion in the lower layers over the Arabian Sea in association with onset of monsoon. The results during third phase correspond typically to break monsoon conditions over the Bay of Bengal. Though the atmosphere has large kinetic energy, there was substantial decrease in moisture contents of the atmosphere, increase in divergence in the lower levels and convergence in upper levels and dominantly downward motion throughout the troposphere. Substantial decrease in the atmospheric moisture contents was also observed during early days of break monsoon period. Another factor noticed was the height of the level of non-divergence which over the Arabian Sea during pre-onset period was around 700 mb and over the Bay of Bengal during the established monsoon period was around 500 mb.

Acknowledgement

The authors are indebted to Shri J. U. Hingorani for his valuable support in providing data and programming advice. We wish to express our gratitude to Shri G. K. Chopra and Shri K. C. Das for preparing diagrams and neat typing respectively.

References

Chowdhuy, M.H.K. and Karmakar, S., 1983, *Mausam,* **34** , 2, pp. 161-166.

Chuchkalov, B.S., 1981, Vertical distribution of average dynamic features over the USSR ship polygons during summer MONEX, International conference on scientific results of monsoon experiment, Bali.

Das, P.K., 1962, Mean vertical motion and non-adiabatic heat sources over India during the monsoon, *Tellus,* **14**, 212-220.

Findlater, J., 1969, Interhemispheric transport of air in the lower troposphere over the western Indian Ocean, *Quart, J.R. Met. Soc.,* **95**, 400-403.

Ghosh, S.K., Pant. M.C. and Dewan, B.N., 1978, Influence of the Arabian Sea on the Indian Summer monsoon, *Tellus,* **30**, 117-125.

Nitta, Tsuyashi, 1980, Preliminary Budget Computations over the Bay of Bengal during summer Monex, Results of the Summer Monex field phase research (Part A), **9**, 145-150.

O' Brien, J.J., 1970, Alternative solutions to the classical vertical velocity problems, *J. appl. Met.,* **9**, 197-203.

Pisharoty, P.R., 1965, Evaporation from Arabian Sea and the Indian southwest monsoon, Proc. Symp. Met. results of International Indian Ocean expedition, Bombay, 22-26.

Ramage, C.S., 1966, The summer atmospheric cirulation over the Arabian Sea, *J. atmos. Sci.,* **23**, 144-150.

Rao, Y.P. and Desai, B.N., 1971, Origin of southwest monsoon current over the Indian seas, *Vayu Mandal,* **1**, 34-36.

Saha, K.R., 1970, Air and water vapour transport across the equator in the western Indian Ocean during northern summer, *Tellus,* **22**, 682-687.

Saha, K.R. and Bavadekar, S.N., 1973, Water vapour budget and precipitation over the Arabian Sea during the northern summer, *Quart., J.R. Met. Soc.,* **99**, 273-278.

Sikka, D.R. and Mathur, M.B., 1965, Transport of water vapour over Arabian Sea during active monsoon situation, Proc. Symp. Met. results of IIOE, Bombay, 55-71.